Efficient and robust wave overtopping estimation for impermeable coastal structures in shallow foreshores using SWASH

Suzuki, Tomohiro; Altomare, Corrado; Veale, William; Verwaest, Toon; Trouw, Koen; Troch, Peter; Zijlema, Marcel

DOI
10.1016/j.coastaleng.2017.01.009

Publication date
2017

Document Version
Final published version

Published in
Coastal Engineering

Citation (APA)
Suzuki, T., Altomare, C., Veale, W., Verwaest, T., Trouw, K., Troch, P., & Zijlema, M. (2017). Efficient and robust wave overtopping estimation for impermeable coastal structures in shallow foreshores using SWASH. *Coastal Engineering*, *122*, 108-123. https://doi.org/10.1016/j.coastaleng.2017.01.009

Coastal Engineering 122 (2017) 108–123

Contents lists available at ScienceDirect

Coastal Engineering

journal homepage: www.elsevier.com/locate/coastaleng

Efficient and robust wave overtopping estimation for impermeable coastal structures in shallow foreshores using SWASH

Tomohiro Suzuki[a,b,*], Corrado Altomare[a,c], William Veale[a], Toon Verwaest[a], Koen Trouw[a,d], Peter Troch[c], Marcel Zijlema[b]

[a] Flanders Hydraulics Research, Berchemlei 115, 2140 Antwerp, Belgium
[b] Dept. of Hydraulic Engineering, Delft University of Technology, Stevinweg 1, 2628 CN Delft, The Netherlands
[c] Dept. of Civil Engineering, Ghent University, Technologiepark 904, 9052 Ghent, Belgium
[d] Fides Engineering, Unitaslaan 11, 2100 Antwerp, Belgium

ARTICLE INFO

Keywords:
SWASH
Wave overtopping
Impermeable coastal structures
Instantaneous overtopping

ABSTRACT

Estimation of wave overtopping over the crest of coastal structures is crucial to design effective and cost efficient countermeasures against storms. Semi-empirical formulas are often used for wave overtopping assessment, but they are not always applicable for complex structures which exist in reality (e.g. a storm wall on a dike in a shallow or very shallow foreshore). Detailed numerical models such as Eulerian and Lagrangian RANS models have potential to simulate overtopping of complex coastal structures with good accuracy. However such models require significant computational resources. The use of such models is often not feasible for the design of coastal structures, which often requires multiple iterations and model runs over a reasonably long period of time (e.g. wave trains with 1000 individual waves). In this paper we investigated the applicability of the simplified depth integrated wave transformation model SWASH for wave overtopping estimation of impermeable coastal structures in shallow foreshores. The validation results demonstrate the capability of SWASH to predict mean wave overtopping discharge with good accuracy compared to results from four different overtopping experimental campaigns (comprising 124 individual cases). The overall performance of SWASH to estimate mean wave overtopping discharge is as accurate as those obtained by semi-empirical equations in literature. However, in order to obtain accurate mean wave overtopping discharge with the SWASH model, the incident wave properties at the toe of the dike need to be accurately reproduced. For cases where this is not possible, a correction method is proposed in this paper. Detailed validation of the instantaneous wave overtopping also shows a good agreement with physical model data. In one example, a single, intensive overtopping event was not well resolved by the SWASH model and the instantaneous wave overtopping was under-predicted. However, this did not contribute significantly to the mean wave overtopping discharge. An additional advantage of the SWASH model is that specific coastal structure geometries can be modelled in SWASH if they are not covered by semi-empirical equations. Even in a case with rapidly varied flow (e.g. vertical wall on a dike) the model shows sufficient robustness. In this paper the details on the SWASH model configuration and post processing methods are outlined to enable the reader to reproduce reliable wave overtopping estimation over impermeable coastal structures in shallow foreshores.

1. Introduction

Prediction of wave overtopping of new and existing coastal structures is an important requirement for those concerned with reducing and monitoring coastal flood risk. Limits of mean tolerable wave overtopping are specified by many regulatory agencies as design criteria which sets the crest level for coastal defences (e.g. Technical Advisory Committee on Water Defences (TAW) in the Netherlands, the Master plan for Coastal Safety in Belgium and, the Environment Agency in the United Kingdom, FEMA in the USA). These limits are specified to avoid structural failure of the existing buildings and to protect people and property in the area behind the coastal structure.

At present the mean rate of wave overtopping for a particular coastal structure, under given wave conditions and water levels, is commonly estimated with (semi-) empirical formulas (e.g. [1,8–12]) or through detailed physical model studies. The validity of formulas and

* Corresponding author at: Flanders Hydraulics Research, Berchemlei 115, 2140 Antwerp, Belgium.
E-mail address: tomohiro.suzuki@mow.vlaanderen.be (T. Suzuki).

http://dx.doi.org/10.1016/j.coastaleng.2017.01.009
Received 9 September 2016; Received in revised form 26 January 2017; Accepted 27 January 2017
Available online 20 February 2017
0378-3839/

physical model results is restricted to specific wave conditions, specific geometries and structure characteristics, related to the laboratory or prototype test configurations. This restriction affects the prediction of wave overtopping at structures that are not well covered in the above mentioned studies, for example overtopping over a sea dike with storm wall in very shallow water conditions.

More recently numerical models have also been used to directly model wave overtopping of coastal structures. Since the overtopping is a nonlinear and stochastic phenomenon, the efforts of engineers and researchers are focused on modelling the entire process that leads to overtopping flows of coastal structures. Besides the mean overtopping discharge, the time series of wave overtopping can be very important to assess local damage or erosive processes on the inner dike slope. However, an accurate estimation of wave propagation, transformation and overtopping by a numerical model is a very challenging task, since the processes involved can be characterized by different scales both in time and in space.

In recent years advances in numerical methods and computer hardware have made it possible to solve the Reynolds-Averaged Navier-Stokes equations (RANS) to model wave overtopping of impermeable sea dikes by implementing Eulerian (e.g. Volume of Fluid method) or Lagrangian (e.g. Smooth Particle Hydrodynamic, Particle Finite Element Method) free surface tracking techniques (e.g. [13–18]) Although RANS models have shown good agreement with physical model results for wave overtopping, these models require advanced numerical modelling skills to implement and are computationally intensive. [19] states that RANS models generally require hours in computation time on a normal PC to simulate seconds of flow in real time. Moreover, the wave boundary in these models is typically set close to the coastal structure to reduce the size of the numerical grid and computational processing time. Even though significant improvements in RANS model speed and resolution has been achieved by the use of GPU techniques (Graphic Processing Unit) instead of CPUs (Central Processing Unit) to run these models (e.g. [20]) detailed modelling still requires significant computational effort in order to represent the entire history of the overtopping phenomena.

On the other hand, a more computationally efficient approach to simulate wave propagation and wave overtopping is adopted with depth integrated models based on the Non-linear Shallow Water Equations (NLSW). [21] first addressed wave overtopping over a sea dike with a numerical model based on the NLSW equations and produced reliable estimation of mean wave overtopping discharge. However, their wave conditions were limited to monochromatic waves. More recent papers based on the NLSW equations (see e.g. [19,22–24]) obtained reasonable mean overtopping discharges for impermeable sea dikes. Nevertheless, these models have limitations due to the assumption of hydrostatic pressure in the NLSW equations. This assumption means that vertical pressure and velocity gradients are not resolved which limits the ability of these models to accurately describe hydrodynamic processes in the swash zone. Finally, other solutions have been developed such as in [25] where the authors present a shock-capturing numerical model, based on the combined solution of Boussinesq and NLSW equations and apply it to the simulation of wave run-up, wave overtopping and wave train propagation over impermeable, emerged and low-crested structures.

There have been many developments for the non-hydrostatic wave-flow models in the last decade (e.g. [26–28]). Those are capable of describing wave propagation over sloping bottoms with a good accuracy. Here we describe a brief comparison over different types of non-hydrostatic models [27,29] and the SWASH model focusing on linear dispersion relation. [27] is based on incompressible Navier-Stokes equations. They applied a Godunov-type scheme and thus the velocities are defined at the cell center and the dynamic pressure is defined at cell faces in order to improve frequency dispersion of waves. In this method a few layers' calculation enables to maintain the linear dispersion relation with a small error. For example their model can maintain relative linear dispersion error within ~2% for the case of kh~3 by a three-layer model. On the other hand the SWASH model can give the relative error ~3% for the case of kh~3 by a one-layer model. The error is slightly higher but ~3% is acceptable and one-layer calculation gives a big advantage. Both methods of [27] and SWASH the vertical flow structure is approximated by means of space discretization of mass and momentum equations. On the other hand, [29] introduced a model based on a semi-integrated approach using integro-differential system. The advantage of the model is that the model can resolve exact linear dispersion relation without relative error. This is achieved by decomposition of the velocity field into a depth averaged one and the deviation. Both models [27,29] were proven to be applicable for wave propagation. However those have not been tested for overtopping estimation.

The objective of this paper is to explore the applicability and limitations of the simplified depth integrated wave transformation model SWASH [30] for efficient wave overtopping estimation at impermeable coastal structures. SWASH is a time-domain wave propagation model based on the NLSW equations with an efficient and stable implementation of a Poisson solver for non-hydrostatic pressure [31]. Cases with a shallow foreshore are tested, and discussions and conclusions are presented.

2. SWASH model

SWASH is an open source deterministic time domain wave model [30]. The governing equations of the model are the non-linear shallow water equations with added non-hydrostatic effects. The one-dimensional, depth-averaged shallow water equations in non-conservative form are shown as follows:

$$\frac{\partial \zeta}{\partial t} + \frac{\partial hu}{\partial x} = 0 \tag{1}$$

$$\frac{\partial u}{\partial t} + u\frac{\partial u}{\partial x} + g\frac{\partial \zeta}{\partial x} + \frac{1}{2}\frac{\partial p_b}{\partial x} + \frac{1}{2}\frac{p_b}{h}\frac{\partial(\zeta - \mathrm{d})}{\partial x} + c_f\frac{u|u|}{h} = 0 \tag{2}$$

$$\frac{\partial w_s}{\partial t} = \frac{2p_b}{h} - \frac{\partial w_b}{\partial t},\ w_b = -u\frac{\partial d}{\partial x} \tag{3}$$

$$\frac{\partial u}{\partial x} + \frac{w_s - w_b}{h} = 0 \tag{4}$$

where t is time, x the horizontal coordinate, u the depth averaged velocity in x-direction, w_s and w_b the velocity in z-direction at the free surface and at the bottom, respectively. ζ is the free-surface elevation from still water level, d is the still water depth and h the total depth. p_b is the non-hydrostatic pressure at the bottom, g the gravitational acceleration and c_f the dimensionless bottom friction coefficient.

The bottom friction coefficient c_f is expressed by Manning's roughness coefficient n as follows:

$$c_f = \frac{n^2 g}{h^{1/3}}. \tag{5}$$

Eqs. (1) and (4) are the global and local continuity equations, respectively, to assure both local and global mass conservation. Eq. (2) is the momentum equation for the u-velocity which includes the effect of non-hydrostatic pressure and bottom friction. Note that momentum conservation is obtained at the discrete level in line with [7]. First equation of Eq. (3) is the momentum equation for the vertical velocity at free surface w_s. The vertical velocity at the bottom w_b is described by means of the kinematic condition as presented by the last part of Eq. (3).

Note that the governing equations are based on the incompressible Navier-Stokes equations when multiple layers in the vertical are considered. In this way we take into account the vertical structure of the horizontal flow. In this study all calculations have been conducted in one single layer, i.e. depth-averaged, which appeared to be sufficient

Table 1
Selected dataset for detailed validation from four physical model campaign.

Dataset id.	N	Scale	Foreshore slope	Dike slope	$H_{m0\text{-}Deep}/h_{toe}$	Schematization (Van Gent [9])	$S_{m\text{-}1,0}$	$h_{toe}/H_{m0\text{-}toe}$	Schematization (Altomare [1])
00-025	11	1/25	1/35	1/2	3.7-28.0	Very shallow	0.0001-0.0004	0.1-0.6	Very shallow
00-142	10	1/25	1/35	1/3	2.3-3.5	Shallow/Very shallow	0.0006-0.0009	0.8-1.0	Very shallow
13-116	85	1/25	1/35	1/3, 1/6	4.9-48.4	Very shallow	0.0001-0.0003	0.0-0.5	Very shallow
13-168	18	1/25	1/50	1/2	0.7-13.4	Intermediate/Shallow /Very shallow	0.0001-0.0033	0.4-1.7	Shallow/very shallow

with respect to frequency dispersion related to wave transformation and suitable for wave overtopping calculation in terms of computational stability.

A full description of the numerical model based on a staggered, conservative, finite-difference scheme, different kinds of boundary conditions, and different types of applications are given in [6,30,32].

3. Experimental data

3.1. Selection of datasets

Four experimental campaigns totalling 124 individual physical model tests, conducted at Flanders Hydraulics Research have been used to validate SWASH modelling for estimating wave overtopping of impermeable coastal structures in shallow foreshores. The main parameters of each campaign setup are listed in Table 1. These data sets are listed as “00-025”, “00-142”, “13-116” and “13-168” in Table 1 and all of these physical model tests were conducted by one of authors in this paper. Those 124 cases used in this manuscript are partly from [1], and the rests are based on original test cases. They can represent overall characteristics since selected overtopping discharge is scattered from small to large.

An overview of the physical model setup for the tests is summarized in [1] and Section 4 of this paper. Note that some data sets used in the present study include cases with storm walls on top of sloping dikes and also a vertical dike on the shallow foreshore. These data sets were not analysed in [1], but are included in the present study to assess the applicability of SWASH to estimate wave overtopping over various impermeable structures in the shallow foreshores. The physical model data sets which have parapets are not included in this paper. As SWASH is a depth integrated model it is not possible to represent parapets geometrically.

The offshore data from the physical model tests was used to create a time series of incident waves using the Mansard and Funke method [33], which was then implemented as the wave boundary in the SWASH model (see details of the implementation in Section 5.1). This approach allowed a direct comparison between the SWASH and physical model test results including wave transformation. As pointed out from e.g. [34,35], the seeding number (i.e. wave train) can make a significant difference in wave overtopping discharge, especially in case of low overtopping rates. In addition, more detailed physical model results (e.g. instantaneous overtopping discharge, video images) were also recorded for some physical model tests to allow further comparison between the SWASH and physical model results.

3.2. Foreshore water levels

Van Gent [9] used the ratio between significant wave height at deep water and water depth at the toe $H_{m0\text{-}Deep}/h_{toe}$ of a coastal structure to categorise foreshore water levels as either ‘deep’, ‘intermediate’, ‘shallow’ or ‘very shallow’. Note that the H_{m0} is calculated from spectral analysis as $4\sqrt{m_0}$. Van Gent (1999) categorized $H_{m0\text{-}Deep}/h_{toe}$=0.4 as ‘deep’, 0.75 as ‘intermediate’, 1.5 as ‘shallow’ and 3.0 as ‘very shallow’. Altomare [1] further indicated that the definition of shallow foreshores and very shallow foreshores can be specified by using as parameters the wave steepness $s_{m\text{-}1,0}$ defined by $2\pi H_{m0}/(g^{*}T_{m\text{-}1,0}{}^{2})$ and the ratio between water depth at the toe and significant wave height at the toe $h_{toe}/H_{m0\text{-}toe}$. When $s_{m\text{-}1,0}$ is smaller than 0.01, the foreshore is considered as shallow or very shallow. Then $h_{toe}/H_{m0\text{-}toe}$ is used to distinguish further, shallow ($h_{toe}/H_{m0\text{-}toe} \leq 1.5$) and very shallow ($h_{toe}/H_{m0} > 1.5$).

In this paper we refer to both methods to check which condition match the test conditions listed Table 1. According to [1,9], the four presented datasets cover a range of intermediate, shallow and very shallow waters. In this paper we emphasize validation of SWASH modelling for wave overtopping in shallow foreshore conditions, as there is a knowledge gap in scientific literature on overtopping of complex or non-conventional structures with shallow and very shallow foreshores. Overtopping of coastal structure with deep and intermediate waters are better covered in existing literature (e.g. [8,10,36]).

3.3. Summary of structural layout and measured properties

Table 2 summarizes the structural layout of each physical model test setup and the measured properties in each campaign. Note that the word ‘dike’ in Table 2 refers to a traditional sloping dike, as opposed to a ‘vertical dike’ which represents a vertical wall. A ‘promenade’ is defined by the 2nd edition of the European Overtopping Manual [37]: ‘*Almost horizontal slopes… situated at a much higher level than a berm in a sloping structure*’. ‘Storm walls’ are also defined by [37] as ‘*a structure that is situated at the top of the vertical wall/dike and the intention is to return the up-rushing wave seawards, decreasing overtopping*’.

Table 2 indicates that a wide range of typical and more complex impermeable coastal structure have been investigated in this paper. To date, berm and wall effect for wave overtopping can be calculated in a deep water condition by an empirical equation [36] but those cannot be calculated if it is in a shallow foreshore condition [1]. The performance of overtopping estimation by SWASH is discussed in this paper for both these conditions.

The incident wave properties (i.e. H_{m0} and $T_{m\text{-}1,0}$) measured at the toe of the dike are typically used in semi-empirical equations (e.g. [8,10]) to estimate mean wave overtopping discharge. However these wave properties are not always available (Table 2). For this reason, total wave properties were also used to evaluate wave condition at the toe of the dike for 00-025. For all the cases the mean wave overtopping discharge was recorded in the physical model tests and are compared against SWASH model estimates in Section 5 of this paper.

Instantaneous wave overtopping discharge was also recorded in some physical model tests (refer to Table 2) along with high-resolution video of the part of the model test. This data is compared with SWASH model estimates in Section 5.2.3 of this paper.

4. Validation with analytical solution

Before investigating the validity of the SWASH model against physical model test data in Section 5, this section briefly compares the model performance against an analytical solution.

4.1. Analytical model

The analytical solution is based on [38], which gives analytical

Table 2
Tested structural layout and measured properties in each physical model campaign.

Dataset id.	Structural layout	Incident wave at the toe of the structure	Total wave at the toe of the structure	Mean wave overtopping discharge	Instantaneous wave overtopping discharge	Video
00-025	Dike/Vertical dike, Promenade, storm wall	No	Yes	Yes	Partly[a]	Partly[a]
00-142	Dike, Promenade	Yes	No	Yes	No	Partly[a]
13-116	Dike, Promenade	Not always applicable	Not always applicable	Yes	Partly[a]	No
13-168	Dike, Promenade, storm wall	Yes	Not applicable	Yes	No	No

[a] "Partly" means that the data is available but only for selected model tests.

overtopping volume over a truncated plane beach using a swash solution. See details in [38].

The total volume of overtopping water per unit width V is expressed as below:

$$V(E) = \frac{1}{27}(4 - 12E + 8E\sqrt{2E} - 3E^2) \quad (6)$$

where E is the relative location of the truncation point on the plane beach. This parameter ranges between 0 and 2, representing run-down point (i.e. starting point of uprush) and maximum run-up point (i.e. starting point of backwash) respectively.

4.2. SWASH model setting

Two SWASH model bathymetries were produced. The length and height of the SWASH model domain was 35 m and 1 m respectively for both cases. The slope of the model bathymetry was 1/35 to represent a plane beach and the grid size in the x-direction was set as 0.02 m for both cases. The plane beach extended to x=35 m in the first model bathymetry, whereas the other model bathymetry was truncated at x = 24 m.

Six regular waves were simulated with the still water level, wave height H and period T equal to 0.6 m, 0.1 m and 10 s, respectively. A weakly reflective boundary condition was prescribed at the upstream wave boundary. The model was run with one layer in the vertical direction and the Manning's n roughness parameter was set to n = 0.000 $s/m^{1/3}$ so that comparison could be made with an analytical solution.

4.3. Comparison with analytical solution

Wave run-up and run-down points were obtained the six simulated waves in the plane beach case. The results are shown in Table 3. This table indicates that a truncation point at x = 24.0 m is always between run-up and run-down points. Mean wave overtopping volume was therefore estimated at this point in the truncated model. Table 3 also shows that after 3 waves the run-up and run-down points stabilise to approximately 22.5 and 25.2 m respectively. Therefore comparison between the SWASH model and the analytical solution is provided for Waves 4 to 6 only.

Table 3 also shows the analytical volume of overtopping wave V estimated at the truncation point E (i.e. x=24.0 m) and the SWASH model predicted overtopping volume. The analytical and simulated wave overtopping estimates for Waves 4 to 6 show relatively good agreement. The wave overtopping results are in the same order of magnitude with the ratio of simulated to analytical overtopping estimates in the range of 0.62 and 1.19. This indicates that SWASH gives credible estimates of mean wave overtopping for a simplified case.

In Section 5 the SWASH model is validated against physical model tests with more complex geometries and more realistic waves.

5. Validation with physical model tests

5.1. Model settings

5.1.1. Physical model set-up and test program

5.1.1.1. Physical model 00-025. The physical model test data of [39] are used to validate the SWASH model for wave overtopping over different kinds of impermeable coastal structures in a shallow foreshore. These tests feature a smooth, impermeable sea dike setup on a concrete foreshore with a constant 1/35 slope (Fig. 1).

Tests were performed at 1/25 scale in the large wave flume at Flanders Hydraulics Research (Antwerp, Belgium). The flume is 70 m long, 1.5 m high and 4 m wide. A piston-type wave generator with a stroke of 0.5 m was used for wave generation with a passive wave absorption system located downstream of the sea-dike. The maximum water depth at the wave generator is 1.2 m. For physical model tests a JONSWAP wave spectrum with γ=3.3 was generated with the wave paddle and the total number of waves generated was about 1000.

Wave height measurements were obtained with twelve resistance type wave gauges installed at the locations summarized in Fig. 1. Mean wave overtopping discharge was obtained by dividing the total volume of water collected in an overtopping box during a test by the total duration of the test. Note that the overtopping box was placed behind the end of the 1/100 promenade except the cases WEN_024 and WEN_026 (refer Table 3) in which the overtopping box is located right behind the dike crest (i.e. without promenade).

Instantaneous overtopping discharge was measured in some selected cases with a Baluff "Micropulse" transducer installed inside the overtopping box situated behind the sea dike. The instantaneous water level reading from the transducer was converted to volume by measuring the difference in water level per overtopping wave and multiplying this number by the dimensions of the overtopping box. The uncertainty in measured mean wave overtopping values in the physical

Table 3
Analytical and numerical overtopping estimation.

Wave #	Run-down, x [m]	Run-up, x [m]	E (x=24.0 m) [–]	V_analytical [l/m]	V_SWASH [l/m]	V_SWASH/V_analytical [–]
Wave 1	–	27.5	–			–
Wave 2	22.8	24.3	1.60	0.6	8.4	13.14
Wave 3	22.2	26.0	0.95	13.8	7.1	0.51
Wave 4	**22.5**	**25.0**	**1.20**	**5.6**	**6.7**	**1.19**
Wave 5	**22.5**	**25.5**	**1.00**	**11.6**	**7.2**	**0.62**
Wave 6	**22.6**	**25.2**	**1.08**	**8.9**	**7.1**	**0.80**

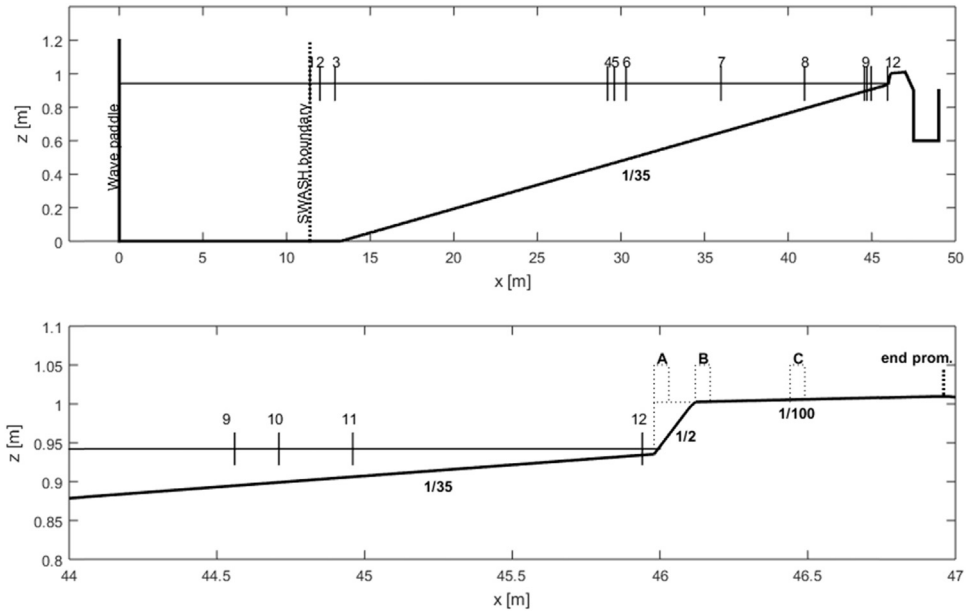

Fig. 1. Physical and numerical model domains for 00-025. Upper panel shows the entire model domain including location of wave gauges 1 to 12. Lower panel shows close up of sea dike and sea wall configuration "A", "B" and "C" with dashed lines.

model due to measurement equipment has been estimated by [39] to be 0.01 ± 0.0005 l/s/m, 0.1 ± 0.001 l/s/m and 1.0 ± 0.025 l/s/m at the 1/25 model scale.

A limitation in this experimental campaign is the use of first-order wave generation and the lack of active wave absorption. However, as proven in [1], the influence of the lack of active wave absorption is negligible. Also, the influence of cross waves was also found to be negligible as detailed in [1]. Note that incident time series estimated from three offshore wave gauges were used in the validations, therefore the first-order wave generation and lack of active wave absorption are not really limitations for those validation cases.

As can be seen in Fig. 1, storm walls are positioned at different location on the dike: 'A' configuration denotes a vertical dike plus a vertical wall immediately behind the 1/35 shallow foreshore slope; 'B' configuration is a 1/2 sloping dike and a vertical wall at the end of the dike slope; and 'C' configuration is a vertical wall in the middle of the dike. The vertical wall was omitted in three test cases (refer as "WEN_004", "WEN_024" and "WEN_026" in Table 3). The mean overtopping discharge for these test cases cannot be estimated by existing semi-empirical equations due to the relatively complex configuration of a promenade combined with a storm wall in a very shallow foreshore. Note that if this were a deep water condition, the equation of [36] could be used to estimate mean wave overtopping discharge, or if the storm wall was not present on the dike the empirical equation introduced by [1] would be applicable.

In total, eleven physical model tests, as listed in Table 4, were simulated with the SWASH model, where H_{m0}, T_p are the offshore measured wave parameters at wave gauge 6 (refer to Fig. 1). The still water levels (SWL) are measured values in the flume before the physical model test began. In these tests the SWL, wave conditions, foreshore level at the toe of the dike, wall heights and dike slopes are varied. Vertical wall elements on top of the dike, at the locations denoted 'A', 'B' and 'C' in Fig. 1, were also tested. Note that the difference in SWL before and after the physical model tests was within 1 mm due to the relatively large volume water in the flume and the relatively small volume of wave overtopping captured inside the overtopping box.

5.1.1.2. Physical model 00-142 and 13-116. The laboratory flume data set of 00-142 and 13-116 are used to validate the SWASH model for wave overtopping over a sloping dike in a shallow foreshore. Those two test regimes were conducted in succession in the same flume at Flanders Hydraulics Research (FHR) using the same offshore bathymetry, wave generation, wave measurement and overtopping measurement methods and only the wave configuration and position of the wave gauges was changed (refer to Fig. 2). Detailed description of these physical model tests are provided in [40] for 00-142 and [1] for 13-116.

Fig. 2 shows an example of the cross section used in 13-116 (case ESF_015, 1/3 sloping dike). The offshore bathymetry used in 00-142 and 13-116 are the same as used in 00-025, with the only exception that the 1/35 slope was terminated at x = 45 m instead of x = 46 m (refer to Fig. 1). Wave generation, wave measurement and overtopping measurement methods were also the same as 00-025 (refer to Section 5.1.1.1). In these case the overtopping box were located behind the crest (no promenade).

In total, ten physical model tests from 00-142 and 86 tests from 13-116 were simulated with the SWASH model.

In the selected cases of 00-142, SWL, dike slope, dike toe level, dike crest level were fixed as 0.960 m, 1/3, 0.910 m and 1.011 m, respectively. Offshore significant wave heights were varied from 0.12 to 0.20 m and offshore peak wave period were varied from 2.0 to 2.4 s.

In the selected cases of 13-116, dike toe level was fixed as 0.910 m and the SWL was varied from 0.9 to 0.935. Tested dike slopes were 1/3 with a dike crest of 1.011 m and 1/6 with a dike crest of 1.015 m. Offshore significant wave heights were varied from 0.12 to 0.24 m and offshore peak wave period were varied from 1.6 to 2.6 s.

5.1.1.3. Physical model 13-168 FHR. The laboratory flume data set of 13-168 (see [1]) are also used for the SWASH overtopping validation. The test uses a smooth, impermeable foreshore with a main slope of 1:50. Fig. 3 shows an example of the cross section used in 13-116 (case REX_014B: 1/2 sloping dike).

In total, 19 physical model tests were simulated with the SWASH model. In the selected cases of 13-168, dike toe level and dike slope were fixed as 0.930 m and 1/2, respectively. SWL was varied from 0.931 to 0.98 m and dike crest level were varied as 0.967 to 1.030 m. Offshore significant wave heights were varied from 0.05 to 0.09 m and offshore peak wave period were varied from 2.2 to 2.6 s.

Table 4
Overtopping test parameters for selected cases (1/25 model scale).

TEST NAME [-]	SWL [m]	Offshore H_{mo} [m]	Offshore T_p [s]	DIKE SLOPE [-]	DIKE TOE LEVEL [m]	DIKE CREST LEVEL[a] [m]	CREST LEVEL [m]	WALL CONFIGRATION [-]
WEN_004	0.942	0.189	2.16	1/2	0.9352	1.0024	1.0096	No wall (Dike+Prom.)
WEN_017	0.989	0.186	2.19	1/2	0.9352	1.0024	1.0504	B
WEN_018	0.989	0.185	2.19	1/2	0.9352	1.0024	1.0504	C
WEN_024	0.967	0.187	2.19	1/2	0.9352	1.0024	1.0676	No wall (only dike)
WEN_026	0.952	0.198	2.63	1/2	0.9352	1.0024	1.0676	No wall (only dike)
WEN_027	0.943	0.196	2.63	1/2	0.9352	1.0024	1.0504	C
WEN_041	0.943	0.188	2.19	1/2	0.9352	1.0024	1.0744	C
WEN_042	0.943	0.186	2.19	1/2	0.9352	1.0024	1.0504	B
WEN_124	0.952	0.186	2.19	0	0.9352	1.0104	1.0343	A
WEN_125	0.952	0.186	2.19	0	0.9352	1.0104	1.0583	A
WEN_126	0.952	0.194	2.19	0	0.9352	1.0104	1.0823	A

[a] at the seaward edge of the dike.

5.1.2. Numerical model setup

Numerical simulations were carried out with SWASH (version 3.14 from swash.sf.net). The physical model layouts described in Section 5.1.1 were reproduced in the SWASH numerical domain. The upstream boundary of the numerical model was delineated at the first wave gauge of the three offshore wave gauges used for incident wave analysis. The total length of the numerical model domain from the upstream boundary to the end of the sea dike was set to the same dimensions as the physical model. In some cases, the basins behind the dike crest were extended in order to provide sufficient volume to collect water overtopping the sea dike. The grid size in the x-direction was set as 0.02 m for all cases. To check the model results are independent of the adopted grid size, sensitivity analysis was conducted (refer to Section 5.2.2.2). The model was run with one layer in the vertical direction since the kd value was less than 1 in all cases, indicating that the estimated phase velocity error is insignificant (where k is the wave number and d the water depth).

The time series of water surface elevation was obtained from incident wave analysis by [33] using the three offshore wave gauges in the physical models. The incident wave time series was prescribed at the wave boundary in the numerical model simulations with a weakly reflective boundary condition [2]. This means that target waves are generated at this boundary however reflected waves from onshore are radiated. A Sommerfeld radiation condition was applied at the downstream end of the numerical domain in order to minimize the effect of the reflection. A still water level was applied as the initial condition for all numerical models tests.

The time duration of the numerical simulations was the same as used in the physical model experiments, approximately 40 min in the model scale to generate 1000 waves. The numerical time step is automatically changed during SWASH calculations to satisfy the Courant–Friedrichs–Lewy (CFL) condition. A Manning coefficient of $n=0.012\ s/m^{1/3}$ was adopted in all numerical simulations after [3,4]. The Manning's n roughness parameter has an influence on mean wave overtopping discharge, particularly when there is a long run-up zone and long berm. For example, in the longest promenade case WEN_004, no bottom friction (i.e. $n = 0.000\ s/m^{1/3}$) gives 40% higher overtopping discharge compared to the original case. A Manning's coefficient of $n = 0.012\ s/m^{1/3}$ was adopted as it represents the smooth wood used in the physical model.

In order to show the basic performance of the SWASH one-layer model, the breaking parameters (see details in [6]) are fixed as default values (i.e. no tuning for wave transformation and overtopping by choosing alternative wave breaking parameters). Note that SWASH accounts for wave energy dissipation even without the breaking parameters due to inherent nature of the shallow water equations (for details see [6,7,42]).

The non-hydrostatic pressure term was applied with a Keller-box scheme, which has significant influence on wave transformation. Explicit time integration was used with a time step restriction set to a maximum Courant number of 0.5 as recommended in SWASH user manual [41].

5.1.3. Post processing

The measured and calculated wave data were post-processed using MATLAB scripts. Time series data was transformed into spectra by Fast Fourier Transform (FFT) algorithms and wave parameters such as H_{m0}, T_p and $T_{m-1,0}$ were calculated. A Hanning window was applied for visualization of the calculated wave spectra. However no smoothing filter was applied to calculated wave parameters. A cut-off frequency of 0.025 Hz was applied for the low frequency waves in order to exclude energy from the resonance frequency of the flume (for further explanation, refer [1]). Note that the resonance from the four test campaigns is very limited, as indicated by minimal scatter in the physical model measurements of significant wave height and period.

5.2. Model results

5.2.1. Wave propagation

5.2.1.1. Example of wave propagation for Model Test 00-025. [30] has previously indicated that the SWASH model can accurately predict the transformation of surface waves in shallow foreshores. This is

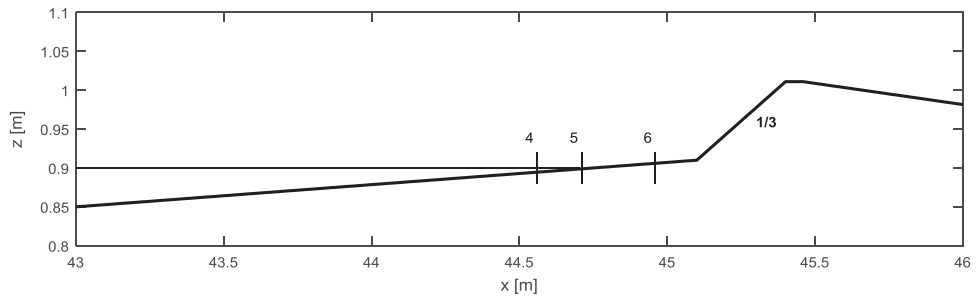

Fig. 2. Physical and numerical model domains close to the dike for 13-116 (case ESF_015, 1/3 sloping dike).

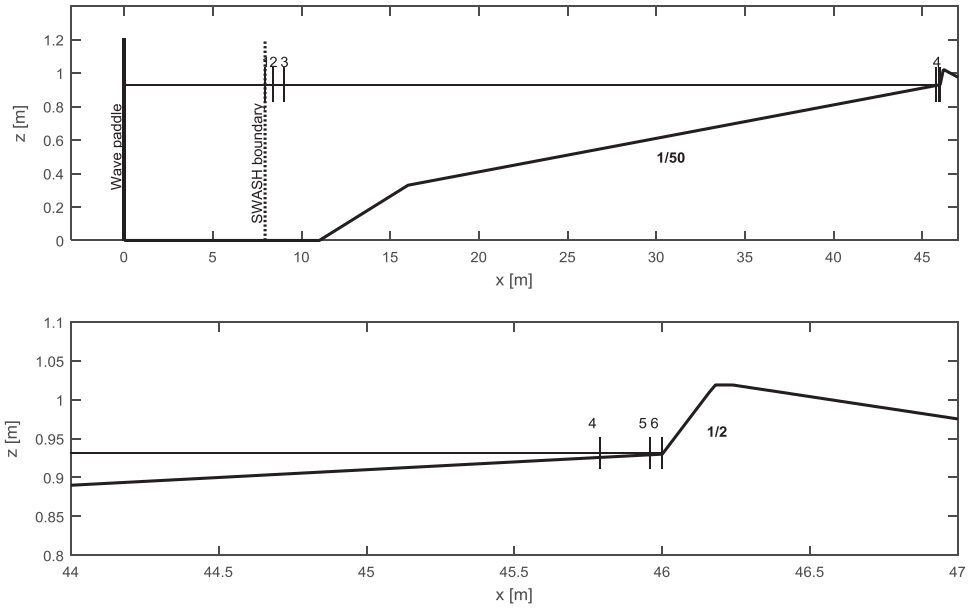

Fig. 3. Physical and numerical model domains close to the dike for 13-168 (case REX_014B: 1/2 sloping dike).

confirmed in Fig. 4 which compares the water surface energy density spectra measured with the physical model and computed by the SWASH model for test WEN_004 at wave gauge No. 3, 5, 7, 8, 10 and 12. No reflection analysis has been performed on these data, and so spectra include both incident and reflected waves.

Fig. 4 indicates that the energy density spectra have almost the same shape to the physical model spectra. The influence of the shallow foreshore is clear from the shape of the spectra, where the well-defined offshore peak has been 'flattened' on the foreshore and energy shifted to low frequencies due to wave breaking and wave-wave interaction. This has been observed in previous studies on wave propagation on shallow foreshores (see e.g. [9,30,43]).

The propagation of wave height (H_{m0}), period ($T_{m-1,0}$) and wave set-up are compared in Fig. 5 between the numerical and physical model, also for test WEN_004. The figure indicates that the SWASH results for significant wave height H_{m0}, period $T_{m-1,0}$ and set-up are in good agreement with data from the physical model. Peak period analysis is not included in this figure as [44] has shown $T_{m-1,0}$ is a more reliable parameter to describe wave overtopping.

Fig. 6 shows the time series of free-surface elevation at wave gauge No. 3, 5, 7, 8, 10 and 12 for test WEN_004. The agreement between the physical and numerical model is generally good. The results are not shown here but similar agreement between physical and numerical model results for wave propagation was found for all model test series 00-025 (refer to Section 5.1.1.1). Here the time series of free-surface

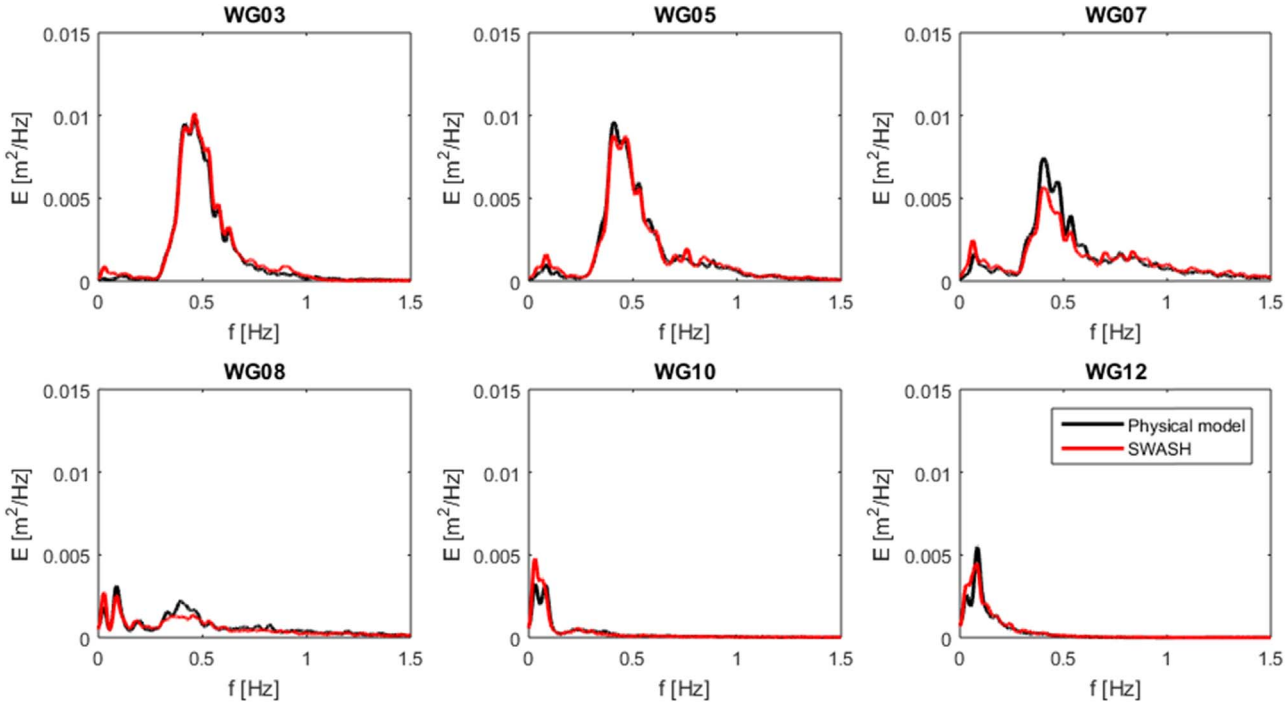

Fig. 4. Water surface energy density spectra measured with physical model (black line) and computed by numerical model (red line) at different stations for test case WEN_004. (For interpretation of the references to color in this figure legend, the reader is referred to the web version of this article.)

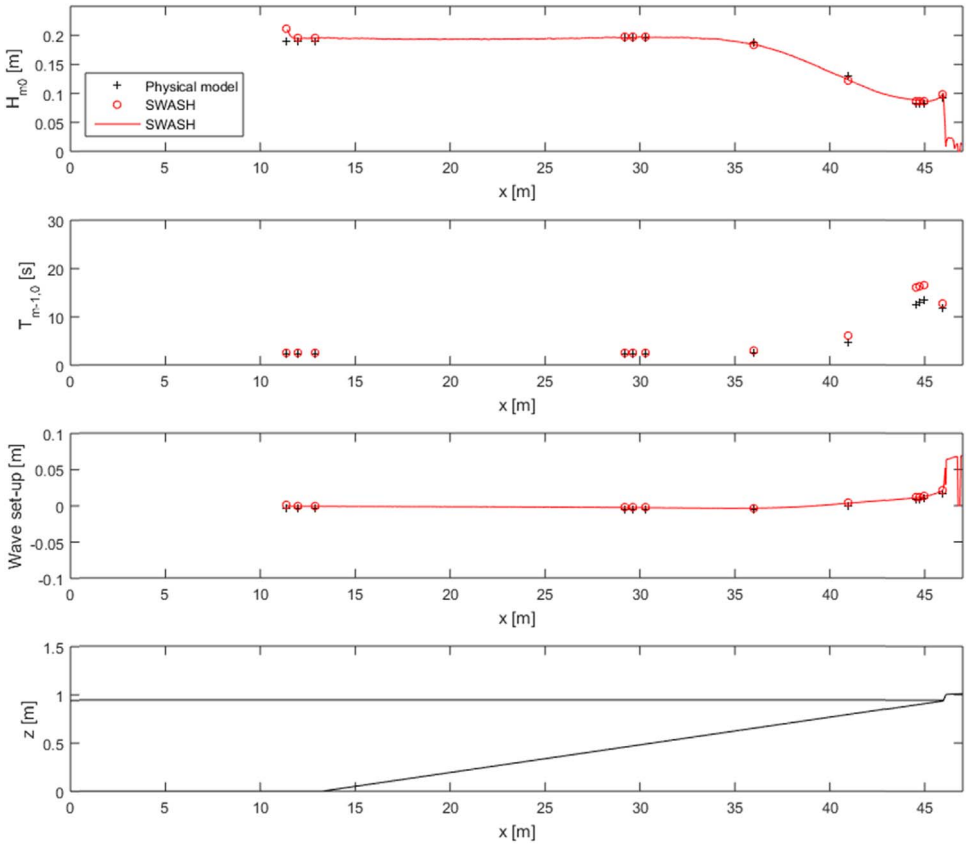

Fig. 5. Significant wave height H_{m0}, wave period, $T_{m-1,0}$, wave set-up measured with physical model (black cross) and computed by SWASH (red circle: post-processed point measurement, red line: processed value inside SWASH calculation) for test case WEN_004.

elevation are also based on the entire wave energy, thus including both incident and reflected waves.

5.2.1.2. Overall wave propagation results. Section 5.2.1.1 indicated that one physical model test (WEN_004 from test series 00-025) simulated with the SWASH model, the setup gave reliable results in terms of significant wave height, spectral wave period and wave set-up. In this section the quality of wave propagation results are investigated for all physical model campaigns.

Table 5 shows the measured and computed total wave H_{m0} and $T_{m-1,0}$ at Ch.12 at the toe of the dike for all tests from dataset 00-025 (refer to Section 5.1.1.1). Here "total wave" refers to the case where incident and reflected waves are analysed together, while "incident wave" refers to where reflected waves are not included in the analysis. In general, predictive formulas for wave overtopping (e.g. [8]) use the incident significant wave height (H_{m0}) and spectral wave period ($T_{m-1,0}$) at the toe of the dike. However, total wave properties are compared in Table 5 as the wave gauge settings at the toe of the dike in the physical model test were insufficient to derive incident wave properties. Note that the wave gauge at Ch. 12 was not used during tests WEN_124, 125 and 126 as the measured data was influenced by significant splashing in front of the vertical dike. For these three cases, the wave height signal at Ch. 11 (instead of Ch. 12) was therefore used for comparison of measured and computed wave properties.

Table 5 shows the comparison of total significant wave height, spectral wave period and set-up. This table indicates that the physical model H_{m0} is well reproduced by SWASH, with an average ratio of $H_{m0\_SWASH}/H_{m0\_Physical\ model}$ = 1.03. Although incident wave properties could not be analysed, the accurate simulation of the total wave properties by the SWASH model indicates that it is likely the incident wave properties are also simulated reliably.

Table 6 shows the measured and computed incident wave H_{m0} and $T_{m-1,0}$ in test campaign 00-142 (refer to Section 5.1.1.2). The estimated incident significant wave height is slightly underestimated (−5%) while the spectral wave period is overestimated (9%). Nevertheless, these differences are relatively small.

In test campaign 13-116 (refer to Section 5.1.1.2), the incident wave properties from the physical model were not always reliable (for reasons outlined in [1]) and therefore not simulated with the SWASH model.

Table 7 shows the measured and computed total wave H_{m0} and $T_{m-1,0}$ in test campaign 13-168 FHR (refer to Section 5.1.1.3). In this case the incident significant wave height is underestimated (−23%) and spectral wave period is overestimated (16%) by the SWASH model.

As long as we compared the wave transformation from the offshore to the toe of the dike in the SWASH model against physical model tests, 1/35 slope cases (very shallow foreshore condition according to [1]) show a good agreement while a 1/50 slope case (shallow/very shallow foreshore condition according to [1]) shows less accurate results. In order to find a better solution for those less accurate cases, two layer mode and different breaking parameter were tested in SWASH. However, none of them improve the results significantly. Yet, main focus of this paper is overtopping behaviour of the SWASH model from toe of the dike, we do not explore this issue further in this paper. Instead, we introduce a correction method for overtopping estimation by using empirical equation in Section 5.2.2. This proposed method will be useful in case one cannot get the target wave at the toe of the dike. Otherwise it is also possible that one can do incident wave calibration at the toe of the dike by changing offshore boundary conditions (see [5]).

Despite the differences for 13-168, the overall results presented in this section indicate that the SWASH model can accurately predict most of the transformation of surface waves in shallow foreshores, and

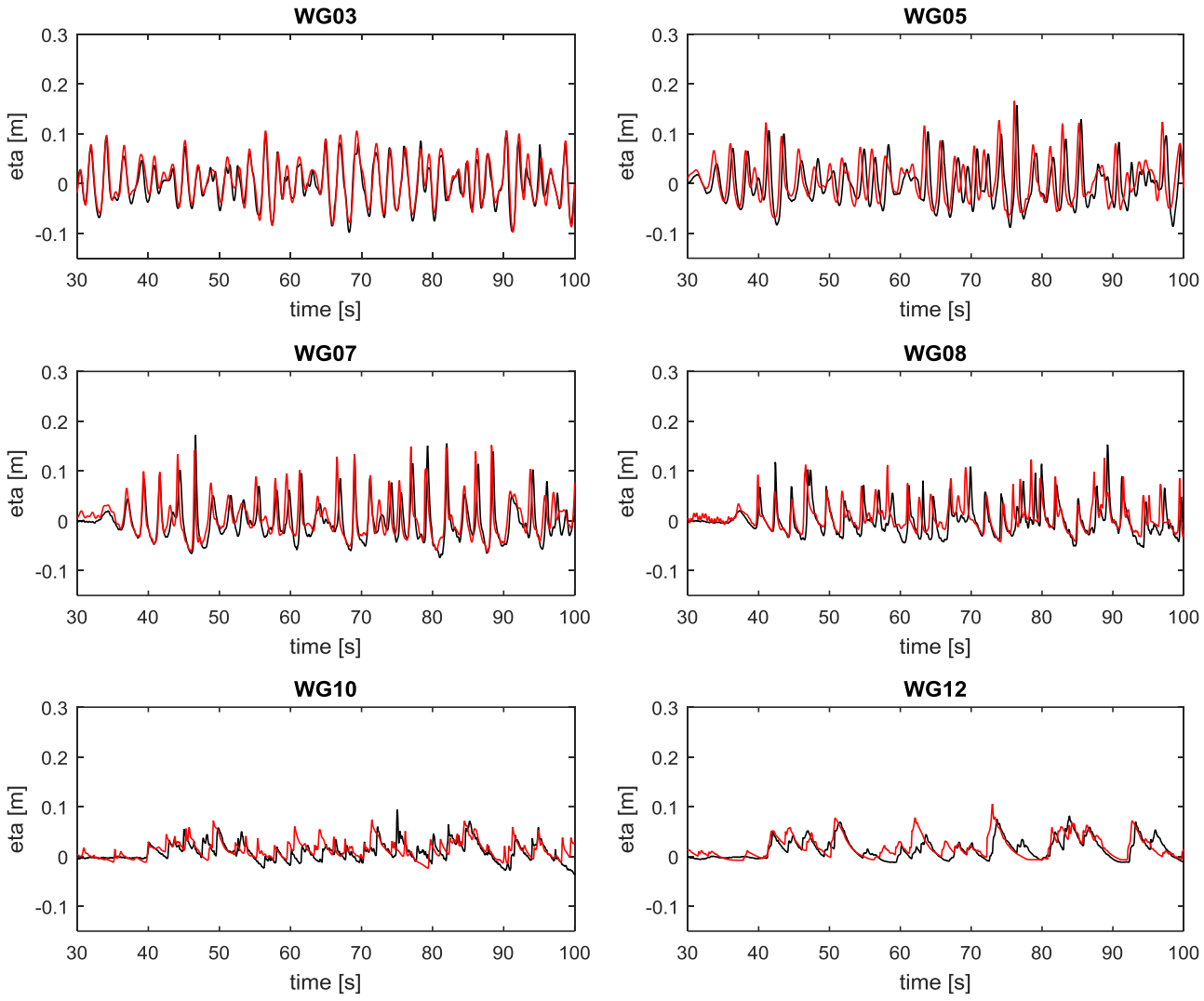

Fig. 6. Time series of water level measured with physical model (black line) and computed by numerical model (red line) at different stations for test case WEN_004. (For interpretation of the references to color in this figure legend, the reader is referred to the web version of this article.)

support the findings of [30]. The capability of the model to predict wave overtopping is evaluated in the following sections.

5.2.2. Mean wave overtopping

5.2.2.1. Overall overtopping calculation results. In this section, the utility of the SWASH model at estimating mean wave overtopping discharge is investigated by comparing measured parameters from the physical model with those computed by the numerical model.

Mean wave overtopping discharge was calculated in the physical model by dividing the total volume of water collected during a test by

Table 5
Measured and computed total significant wave height H_{m0}, spectral wave period $T_{m-1,0}$ and wave set-up (id: 00-025).

Test cases	Physical model			SWASH			Ratio H_{m0}	Ratio $T_{m-1,0}$	Diff. set-up
	H_{m0} [m]	$T_{m-1,0}$ [s]	Set-up [m]	H_{m0} [m]	$T_{m-1,0}$ [s]	Set-up [m]	H_{m0_S}/H_{m0_P} [−]	$T_{m-1,0\_S}/T_{m-1,0\_P}$ [−]	Diff. [m]
WEN_004	0.093	11.75	0.017	0.098	12.7	0.022	1.05	1.08	0.004
WEN_042	0.095	11.91	NaN	0.101	11.24	0.021	1.07	0.94	NaN
WEN_027	0.093	11.89	0.017	0.097	11.66	0.021	1.04	0.98	0.004
WEN_041	0.096	11.94	NaN	0.097	11.65	0.021	1.02	0.98	NaN
WEN_017	0.123	9.36	0.010	0.128	9.41	0.014	1.04	1.01	0.004
WEN_018	0.113	10.57	0.010	0.118	10.41	0.014	1.04	0.98	0.004
WEN_124[a]	0.091	12.48	0.010	0.090	12.91	0.012	0.99	1.03	0.003
WEN_125[a]	0.092	12.36	0.019	0.091	13.41	0.012	0.99	1.08	−0.007
WEN_126[a]	0.092	12.38	0.010	0.089	12.64	0.012	0.97	1.02	0.002
WEN_026	0.096	11.36	0.017	0.103	11.23	0.021	1.07	0.99	0.004
WEN_024	0.114	10.51	0.014	0.119	10.26	0.016	1.04	0.98	0.002
						Ave.	**1.03**	**1.01**	**0.002**

[a] Ch11 were used for those test cases.

Table 6
Measured and computed incident wave H_{m0} and $T_{m-1,0}$ at the toe of the dike (id: 00-142).

Test cases	Physical model			SWASH			Ratio H_{m0}	Ratio $T_{m-1,0}$	Diff. set-up
	H_{m0} [m]	$T_{m-1,0}$ [s]	Set-up [m]	H_{m0} [m]	$T_{m-1,0}$ [s]	Set-up [m]	H_{m0}/H_{m0} [-]	$T_{m-1,0}/T_{m-1,0}$ [-]	Diff. [m]
OWF_134	0.061	6.94	0.006	0.059	7.57	0.004	0.96	1.09	−0.002
OWF_135	0.061	6.91	0.007	0.058	7.38	0.004	0.95	1.07	−0.004
OWF_143	0.065	7.58	0.007	0.062	7.80	0.004	0.95	1.03	−0.003
OWF_144	0.065	7.57	0.007	0.062	7.96	0.004	0.95	1.05	−0.003
OWF_153	0.069	8.09	0.007	0.065	8.25	0.004	0.94	1.02	−0.003
OWF_164	0.051	4.88	0.003	0.049	5.92	0.002	0.96	1.21	−0.001
OWF_174	0.054	5.46	0.003	0.051	6.34	0.002	0.95	1.16	−0.001
OWF_187	0.057	5.87	0.004	0.054	6.80	0.002	0.95	1.16	−0.002
OWF_189	0.058	6.09	0.004	0.054	6.31	0.002	0.94	1.04	−0.001
OWF_188	0.058	6.21	0.004	0.055	6.65	0.002	0.95	1.07	−0.002
						Ave.	**0.95**	**1.09**	**−0.002**

the total duration of the test. In the numerical model a time series of overtopping layer thickness, h(t), and overtopping velocity, u(t) on the sea dike or on top of the wave wall was extracted at the crest point. The point of overtopping estimation in the numerical model and the overtopping box in the physical model is around or less than 1 m, therefore the time lag is not significant. The overtopping rate q(t) per unit length was then calculated as the product of overtopping layer thickness and overtopping velocity, refer to Eq. (7). Mean wave overtopping discharge is calculated by integrating q(t) over the test duration, see Eq. (8), where t_i and t_f are the respective start and end time of the wave overtopping discharge measurements.

$$q(t) = h(t)u(t) \tag{7}$$

$$\bar{q} = \frac{\int_{t_i}^{t_f} q(t)dt}{t_f - t_i} \tag{8}$$

Mean wave overtopping shows significant scatter when the absolute overtopping discharge is relatively small. When the absolute value of the overtopping discharge is small, the number of overtopping waves is generally also small and the mean overtopping discharge can be strongly influenced by a few overtopping events (e.g. [34]).

Fig. 7 plots the measured mean wave overtopping discharge from the physical and SWASH models. Generally, the mean overtopping discharge estimated by SWASH model show a good agreement with physical model test results. For reasons outlined previously, the discrepancy between the SWASH and physical model results is relatively small when overtopping discharge is large and vice versa. Note that the dashed lines in Fig. 7 indicate a factor of three. SWASH is capable to reproduce the physical model mean overtopping discharge reasonably well when it is over 0.01 l/s/m (i.e. over 90% of the data are within the dashed lines). On the other hand the scatter becomes bigger below 0.01 l/s/m, although the general scatter is around 1:1 line.

Table 8 shows the result of prediction performance by the SWASH model estimated by geometric mean (Geo) and geometric standard deviation (GSD). Geo is 0.80 and GSD is 2.49, which is comparable with values obtained in [1]. For definition of Geo and GSD the reader can refer to [10].

[1] suggested an empirical equation for wave overtopping in shallow foreshores by using the equivalent slope concept. This model is used to modify overtopping discharges predicted by the SWASH model. The modification is calculated by the equation below:

$$q_{SWASH\_MOD} = q_{SWASH}\frac{q_{eq\,(input:incident\ wave\ properties\ from\ physical\ model)}}{q_{eq\,(input:incident\ wave\ properties\ from\ SWASH)}} \tag{9}$$

Fig. 8 shows modified overtopping discharge for tests where it was applicable (i.e. test series 00-142 and 13-168 where incident wave properties (i.e. H_{m0} and $T_{m-1,0}$) in physical model were available). After the modification, the performance is improved slightly. As expected, the results for test series 00-142 were modified very little since the incident wave estimation by SWASH was almost the same as measured

Table 7
Measured and computed incident wave H_{m0} and $T_{m-1,0}$ at the toe of the dike (id: 13-168 FHR).

Test cases	Physical model			SWASH			Ratio H_{m0}	Ratio $T_{m-1,0}$	Diff. set-up
	H_{m0} [m]	$T_{m-1,0}$ [s]	Set-up [m]	H_{m0} [m]	$T_{m-1,0}$ [s]	Set-up [m]	H_{m0}/H_{m0} [−]	$T_{m-1,0}/T_{m-1,0}$ [−]	Diff. [m]
REX_014B	0.031	10.64	0.007	0.024	11.78	0.009	0.78	1.11	0.002
REX_014C	0.031	10.64	0.007	0.024	11.78	0.009	0.78	1.11	0.002
REX_015B	0.035	11.19	0.007	0.027	12.04	0.010	0.79	1.08	0.002
REX_015C	0.035	11.19	0.007	0.027	12.04	0.010	0.79	1.08	0.002
REX_035B	0.046	8.31	0.003	0.035	9.74	0.002	0.77	1.17	0.000
REX_036B	0.039	6.22	0.001	0.028	8.02	0.001	0.73	1.29	0.000
REX_036C	0.039	6.22	0.001	0.028	8.02	0.001	0.73	1.29	0.000
REX_039B	0.030	11.18	0.007	0.024	12.06	0.009	0.80	1.08	0.002
REX_039C	0.030	11.18	0.007	0.024	12.06	0.009	0.80	1.08	0.002
REX_39bB	0.030	11.03	0.007	0.024	12.10	0.009	0.82	1.10	0.002
REX_39bC	0.030	11.03	0.007	0.024	12.10	0.009	0.82	1.10	0.002
REX_0e1B	0.039	6.80	0.001	0.030	8.38	0.001	0.76	1.23	0.000
REX_0e3B	0.032	5.23	0.000	0.024	6.90	0.001	0.75	1.32	0.000
REX_060B	0.045	4.66	−0.001	0.035	5.87	0.001	0.77	1.26	0.001
REX_085B	0.047	5.07	−0.001	0.037	6.20	0.001	0.79	1.22	0.002
REX_097B	0.046	8.42	0.003	0.035	9.90	0.002	0.76	1.18	−0.001
REX_097C	0.046	8.42	0.003	0.035	9.90	0.002	0.76	1.18	−0.001
REX_105B	0.030	11.21	0.007	0.023	12.00	0.009	0.76	1.07	0.002
REX_105C	0.030	11.21	0.007	0.023	12.00	0.009	0.76	1.07	0.002
						Ave.	**0.77**	**1.16**	**0.001**

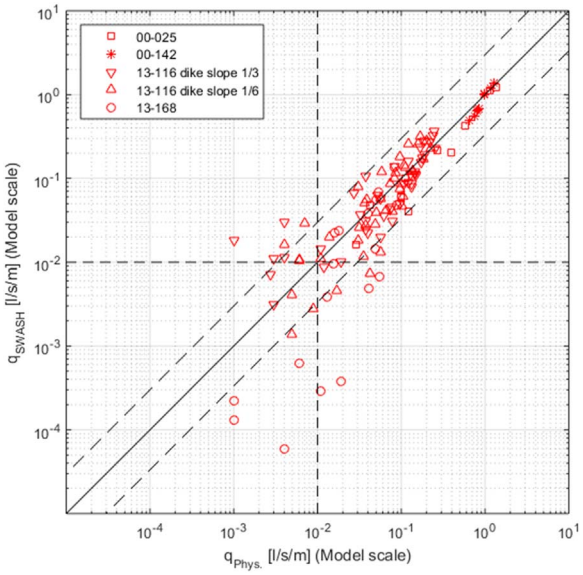

Fig. 7. Measured and computed mean wave overtopping discharge (1/25 model scale) for shallow water condition (without modification).

Table 8
Result of prediction performance by the SWASH model for shallow foreshore case estimated by Geo and GSD (not modified values and modified values by [1]).

Dataset id.	N (Not modified)	Geo (Not modified)	GSD (Not modified)	Geo (Modified)	GSD (Modified)
00-025	11	0.70	1.40	–	–
00-142	10	0.89	1.15	0.99	1.19
13-116 slope 1/3	42	1.11	2.12	–	–
13-116 slope 1/6	43	0.95	2.04	–	–
13-168	18	0.26	4.35	0.63	4.81
Total	**124**	**0.80**	**2.49**	**0.92**	**2.36**

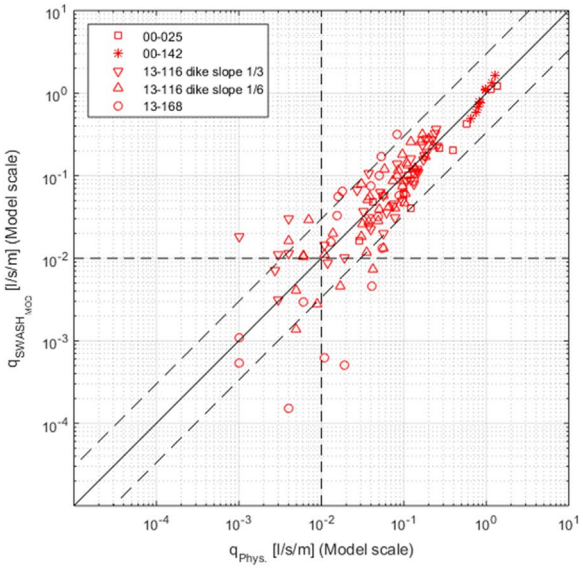

Fig. 8. Measured and computed mean wave overtopping discharge for shallow water condition (with modification).

in the physical model. For 13-168, the modification results in an increase in most of the overtopping discharge values since the incident wave heights were underestimated by the SWASH model. This result can be also seen in Table 8, where the Geo values are improved if the modification is applied.

It can be concluded that the SWASH model can reproduce the mean wave overtopping discharge reasonably well for values greater than 0.01 l/s/m in the 1/25 scale models, with the accuracy of estimation by the SWASH model within a factor of 1 to 3 of the actual overtopping discharge. This result is equivalent or even better in terms of accuracy to semi-empirical equations (e.g. [1,8,10]) developed to assess mean wave overtopping. For instance [8] stated that empirical equations give, at best, a factor of 1 to 3 of the actual overtopping rate.

5.2.2.2. Sensitivity of grid size. As shown in the previous section, SWASH is capable of estimating wave overtopping discharge with a certain accuracy under specified tested conditions. However, the performance of estimating mean overtopping discharge can depend on the model settings. A key issue regarding the SWASH model is the settings to use in order to provide reliable results while maintaining realistic computational run-times. In this regard, the model grid size plays an important role. In general, results from the SWASH model are more accurate when the grid is finer at the expense of computational run-time. In this section, a sensitivity analysis on the grid size is conducted for model test series 00-025 (refer to Section 5.1.1.1).

Fig. 9 shows that the performance of mean wave overtopping discharge (q_SWASH/q_Phys) estimated for test campaign 00-025 as a function of a non-dimensional parameter, wave length at the toe over grid size (L/dx). The wave length at the toe is calculated by $T_{m-1,0}\sqrt{g(d + H_{m0})}$, based on the solitary wave model. The grid size is varied from 0.01 to 0.08 m. The results are not shown in Fig. 9, but the incident significant wave height were almost the same for all grid sizes tested, H_{m0} = 0.090 (dx = 0.01 m), 0.091 (dx = 0.02 m), 0.091 (dx = 0.04 m), 0.091 m (dx = 0.08 m), respectively. This implies that the grid size does not have so much influence on the wave transformation. However, Fig. 9 shows that the performance of the mean overtopping estimation is somewhat sensitive to the non-dimensional parameter L/dx. The L/dx value less than 200 gives lower overtopping discharge. It is underlined that all L/dx values used in the Section 5.2.2.1 were more than 200.

5.2.3. Instantaneous wave overtopping

Instantaneous wave overtopping was derived from the numerical model using the methodology previously described in Section 5.2.2. The free surface elevation, overtopping layer thickness, overtopping velocity and overtopping discharge rate are plotted in Fig. 10 for test

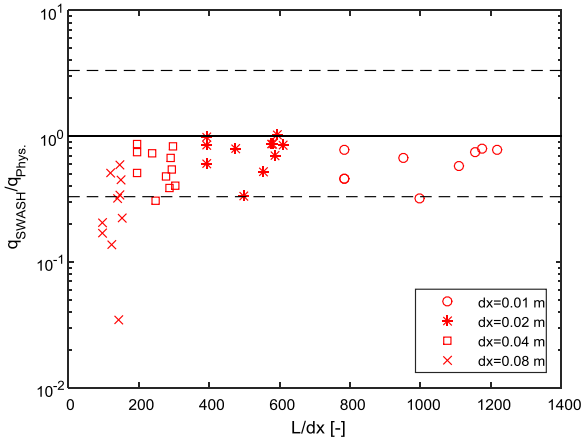

Fig. 9. Ratio of the mean wave overtopping discharge (q_SWASH/q_Phys.) versus L/dx.

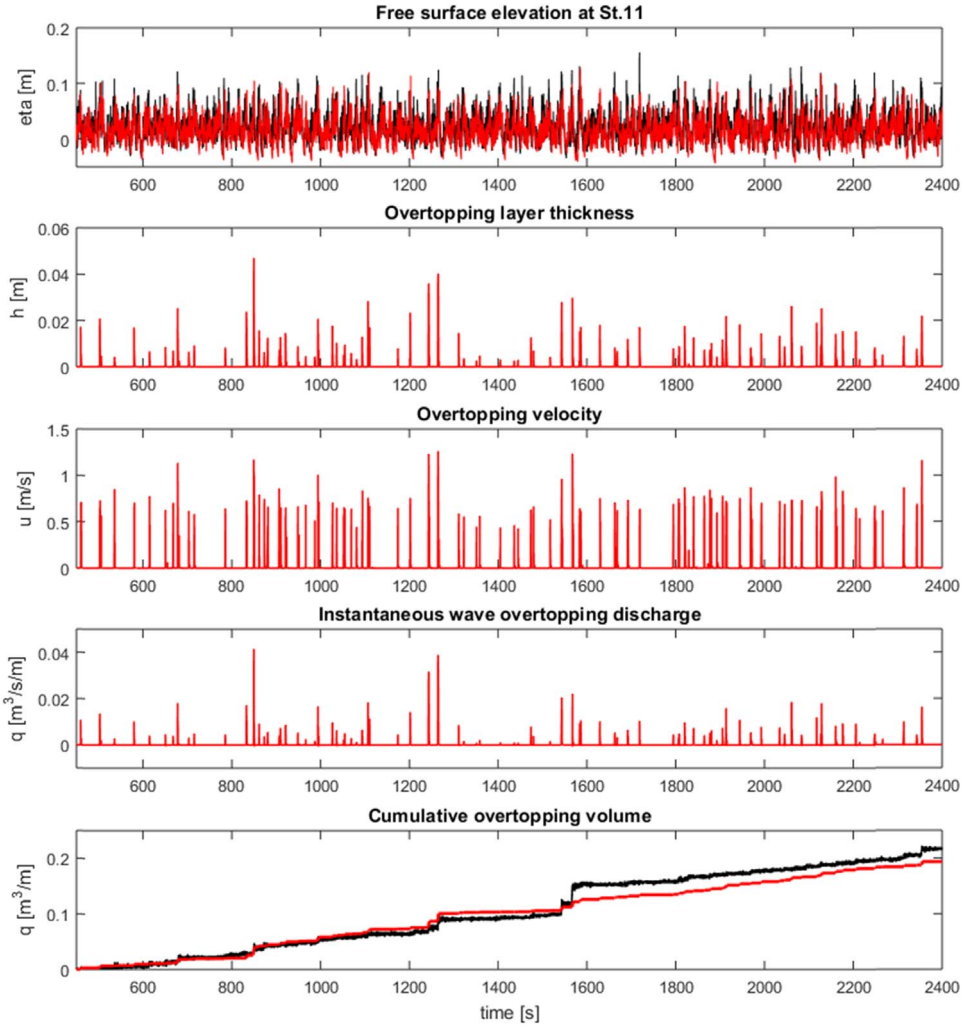

Fig. 10. Measured (black line) and computed (red line) free surface elevation, computed overtopping layer thickness, computed overtopping velocity, computed instantaneous overtopping discharge and measured and computed cumulative overtopping volume for test WEN_125. (For interpretation of the references to color in this figure legend, the reader is referred to the web version of this article.)

WEN_125. WEN_125 has been chosen because instantaneous overtopping discharge was measured for the total duration of the test and video images are available. The free surface elevation at WG.12 (at the dike toe position) was not available for this test and WG.11 has been used instead. Cumulative wave overtopping volume V(t) has also been derived from integration of q(t) from the numerical model and plotted in the bottom pane of Fig. 10 for both the physical and numerical models. Derivation of the cumulative wave overtopping volume in the physical model was calculated by converting the water level measured in the overtopping box to volume.

Comparison of the cumulative wave overtopping in Fig. 10 reveals that the numerical and physical model closely match one another in terms of the trend of wave by wave overtopping when the same time series from the physical model is prescribed in the numerical model. However the largest overtopping wave, occurring at approximately t = 1560 – 1570 s, is underestimated by the numerical model. The cumulative wave overtopping was affected by single intense event that the SWASH model is unable to resolve. The ratio of the discharge of the single intense event to the total overtopping discharge was 14%. The influence of the single event to the average overtopping discharge was limited to only one event and this 14% difference can be acceptable.

To understand the ability of the numerical model to resolve single intense overtopping events, the water surface elevation predicted by the numerical model in front of the sea dike is compared qualitatively using video images against the physical model for the large overtopping waves in the physical model, occurring around t = 1270 s and t = 1560 s. Fig. 11 shows one of the large overtopping cases around t = 1270 s, and Fig. 12 shows the largest overtopping case around t = 1560 s. Those figures illustrate the solitary bores which are generated through wave grouping processes occurring on the shallow foreshore. Such bores have the potential to produce significant wave overtopping of the vertical dike.

Fig. 11 demonstrates that the SWASH model captures the water surface well. This is also explained by the time series of cumulative overtopping discharge shown in the bottom pane of Fig. 11. Note that the vertical dike simulated in the SWASH model was slightly wider than physical model wall in order to get stable overtopping layer thickness and overtopping velocity data from the SWASH model. However this does not have a significant influence on the overtopping results. The wall width represented in the SWASH model is shown with a red line in the top pane of Figs. 11 and 12.

The top and bottom panes of Fig. 11 show, 1) a solitary bore approaching the vertical dike, 2) impact and wave separation at the vertical dike, 3) overtopping and reflection and 4) overtopping and a return wave. In the bore approach phase, the free surface level simulated by the SWASH model is almost identical to the physical model. However the SWASH model does not model the wave separation phase perfectly because it is a depth integrated model, and hence slightly underestimates the water surface profile at the moment of wave separation. After the wave separation (splash), a part of the wave starts

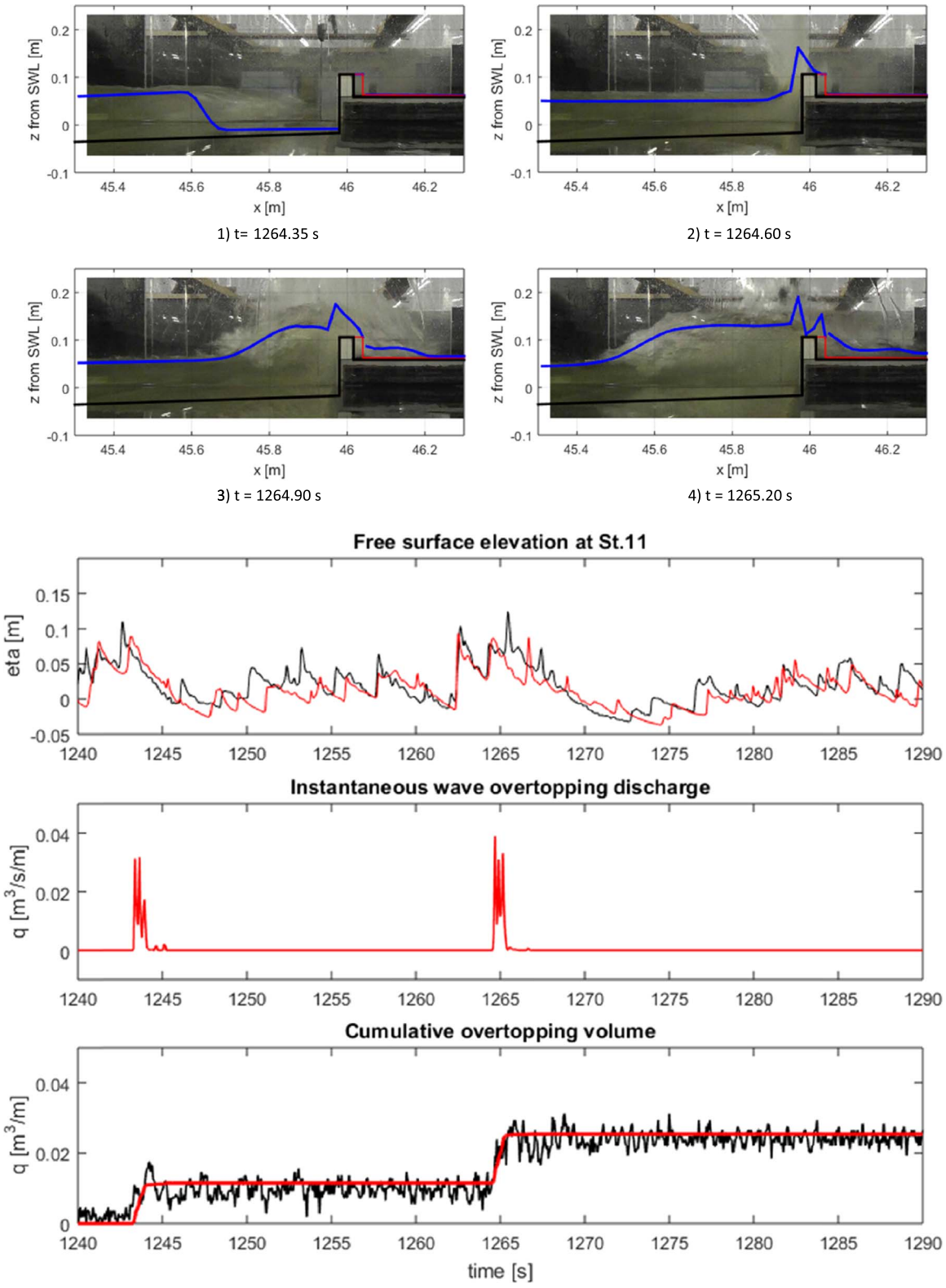

Fig. 11. [Top pane] Physical model image and numerical model calculation (blue line). Black line shows bathymetry and structure while red line behind the seawall shows bathymetry used in SWASH. [Bottom pane] Measured (black line) and computed (red line) time series of water surface elevation at WG.11, computed instantaneous overtopping discharge and measured and computed cumulative overtopping discharge between 1240 to 1290 s of large overtopping wave from test of 1000 waves for test case WEN_125. (For interpretation of the references to color in this figure legend, the reader is referred to the web version of this article.)

overtopping over the wall, and the remaining portion of the wave is reflected. The simulated free surface of the overtopping wave behind the vertical dike seems to be almost identical to the physical model. However there is significant air-entrainment in the reflected wave of the physical model. The SWASH model does not represent such air-entrainment and appears to underestimate the water surface profile of the reflected wave. However, overall results show good qualitative agreement with the physical model in this case.

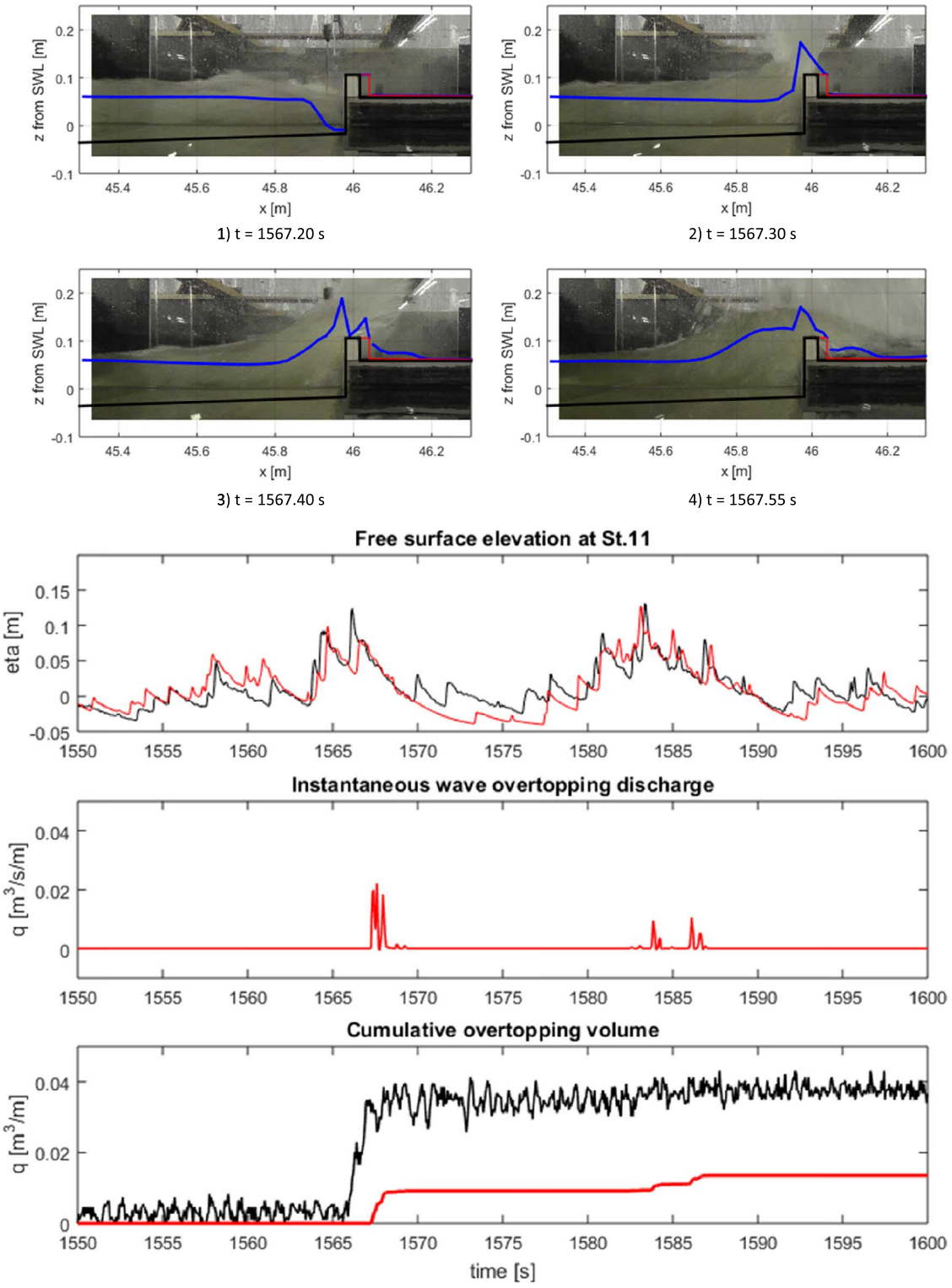

Fig. 12. [Top pane] Physical model image and numerical model calculation (blue line). Black line shows bathymetry and structure while red line behind the seawall shows bathymetry used in SWASH. [Bottom pane] Measured (black line) and computed (red line) time series of water surface elevation at WG.11, computed instantaneous overtopping discharge and measured and computed cumulative overtopping discharge between 1550 to 1600 s (bottom pane) of largest overtopping wave from test of 1000 waves for test case WEN_125. (For interpretation of the references to color in this figure legend, the reader is referred to the web version of this article.)

On the other hand, Fig. 12 shows a case in which SWASH model does not accurately predict overtopping of a specific solitary bore. In this case, the free surface level simulated by the SWASH model in the solitary bore approach phase is already underestimated compared to the physical model. The complex physical processes inherent in the formation, propagation and overtopping of these solitary bores is not always exactly reproduced by the numerical model. Hence the overtopping volume predicted by the numerical model was underestimated.

It can be concluded that SWASH is capable of predicting the instantaneous wave overtopping if the wave time series are correctly reproduced. Even though wave parameters are matched (e.g. H_{m0_SWASH}/H_{m0_Phys} = 0.99 in the tested case WEN_125) it cannot

be guaranteed that all instantaneous wave overtopping events are well reproduced since wave time series can differ from the one in physical model test. For low overtopping discharge small difference can lead relatively large difference in the ratio.

6. Discussion

6.1. Quality of incident waves and overtopping estimation

In order to estimate wave overtopping discharge over an impermeable structure, it is important that a numerical model can reproduce the wave transformation from offshore to the target location (typically at or near the toe of the structure). The results described in Section 5.2 indicate that the SWASH model is generally capable accurately of reproducing wave properties such as H_{m0} and $T_{m-1,0}$ as well as the wave spectrum, wave set-up and time series of water surface elevation at the target location (with the exception of test series 13-168).

A key to success for estimating reasonable overtopping discharge by the SWASH model is the quality of the incident wave property estimates at the toe of the dike. In test series 00-025 and 00-142, the incident wave properties at the toe of the dike were estimated with a very small error (within 5% and with Geo = 0.7, GSD = 1.4 for 00-025; Geo = 0.89, GSD = 1.15 for 00-142). For test series 13-168 the incident wave properties at the target location measured in SWASH are not as well matched to those measured in the physical model. It is possible to correct SWASH predicted incident wave properties with empirical equations (e.g. [6]). However, this artificial manipulation introduces more uncertainty, especially when the mean wave overtopping discharge is small. Adjusting wave properties is not always the best solution since especially wave-wave interaction around the toe is highly non-linear, however, this manipulation is useful to correct at least Geo value.

As shown in Section 5.2.3, SWASH not only gives reliable mean wave overtopping discharge but also represents instantaneous wave overtopping well. Estimated values of Geo=0.92 and GSD=2.36 indicate that the SWASH model predicts the mean wave overtopping value very well and, 90% of the population of the data is within a factor of 3.9 (=1.64*GSD). This indicates that the SWASH model under specified settings used in this paper is able to accurately estimate mean wave overtopping discharge over impermeable coastal structures when mean wave overtopping discharge is greater than 0.01 l/s/m at 1/25 scale. Using Froude number similarity, 0.01 l/s/m at 1/25 scale can be translated to approximately 1 l/s/m at prototype scale.

Note that experimental sensitivity can play an important part in the poor performances of SWASH at low discharges. Further, at low discharges surface tension (not modelled by SWASH) and bed friction (poorly modelled near the shoreline, see [45]) will have an important bearing on the experimental overtopping.

6.2. Limitations of the model

Since SWASH is a depth integrated model, any configuration which has more than two solids in the vertical direction (e.g. parapet) cannot be applied. Additionally, overturning (e.g. plunging waves), separation due to splash and air-entrainment are not represented in the model due to the same reason. However, wave dissipation due to wave breaking is reasonably well represented due to the shock capturing feature and the hydrostatic front approximation ([6,7]) implemented in the SWASH model. Regarding air-entrainment, SWASH may represent prototype scale tests more accurately as physical model tests tend to have more air entrainment compared to in situ tests.

In order to design coastal structures safety it is recommended to repeat SWASH calculation with different wave seeding numbers (i.e. multiple different random wave trains). This is not limited to SWASH, but also for physical model and other numerical models. SWASH has an advantage for such repetitive simulations as the model is not computationally expensive and provides good accuracy for wave transformation and overtopping as shown in Section 5.2.

The restriction of a one dimension model is that it implicitly assumes that the section of foreshore and coastal structure is alongshore-homogeneous and that waves are shore-normal and there is no directional spreading effect for wave transformation.

6.3. Efficiency of overtopping calculation

One of the most important topics in this paper is not only the accuracy but also the model efficiency. As an example of the SWASH model simulation time, the model simulation time for a one layer calculation of 1000 waves for test WEN_004 took approximately 20 minutes to simulate on a PC with an Intel Xeon CPU 2.67 GHz. A two-layer simulation took approximately 3 hours. Note that the calculation using SWASH can be accelerated when parallel computation is used.

Accuracy and computational speed have a trade-off relationship. For example, in WEN_004, a two layer calculation gives slightly better result for the mean wave overtopping (about 20% closer to the measured result), however the computational cost is increased and robustness is decreased.

Theoretically SWASH is not the most accurate model for the estimation of wave overtopping. VOF and SPH models might be able to reproduce better results since they contain a higher vertical resolution than SWASH. However for engineering purposes it is practical to have a model which is not too computationally expensive. For example, wave overtopping test durations are typically relatively long (e.g. 1000 waves) and a number of wave trains are required to be simulated. It is beneficial in such cases to have a model with a relatively low computational cost such as SWASH.

7. Conclusions

In total 124 individual tests from four different physical model campaigns have been used to evaluate the SWASH model for estimating wave overtopping for impermeable coastal structures in shallow foreshores.

SWASH model results were initially compared to the analytical solution of [38]. The SWASH model results showed a good agreement with the analytical solution for a simple case of regular waves overtopping on a truncated beach. This result confirmed the basic performance of the SWASH model against a benchmark test.

The SWASH model was then used to reproduce physical model tests of wave overtopping in (very) shallow water, conducted at Flanders Hydraulic Research laboratory. Comparison between the model predicted and measured data from the physical model tests demonstrated the capability of SWASH to predict mean wave overtopping discharge with good accuracy for shallow water cases when the mean wave overtopping is greater than ~1 l/s/m in the prototype scale. As for the wave transformation from the offshore to the toe, the 1/50 slope case shows less accurate results compared to the 1/35 slope cases. For cases where the incident wave properties are not accurately modelled, a correction method is proposed in this paper. The overall performance of the numerical estimations of the mean wave overtopping discharge is as accurate as the one obtained by semi-empirical equations from literature and the model is sufficiently robust when one layer is applied.

The SWASH model was also shown to be generally capable of predicting the instantaneous wave overtopping from single wave overtopping events if incident wave time series are correctly reproduced. In one example, a single overtopping event was not resolved well by the SWASH model due to the errors when estimating the incident wave time series. However, this did not contribute significantly to the mean wave overtopping discharge. For relatively small overtopping cases (e.g. less than 1 l/s/m), small difference in incident wave time series (especially on the peak level) can lead a significant difference in overtopping.

The settings of SWASH and overtopping characteristics were also discussed and model limitations and calculation efficiency were described.

Although there are limitations with SWASH (primarily as it is a depth integrated model as outlined in Section 6.2), the accuracy and efficiency of the model means it can be reliably applied to estimating wave overtopping discharge over impermeable structures in a shallow foreshore. A combination of semi-empirical equations and SWASH modelling provides engineers and scientists with an efficient and robust tool for estimating overtopping of such structures.

Acknowledgements

The authors express appreciation to STW-project 12176 and Dr. Xuexue Chen to provide physical model data for the overtopping validation (dataset id 00-142). The authors also thank Julien De Rouck for the discussion and advices, and Tim Spiesschaert for the dedicated work conducted at Flanders Hydraulics Research.

References

[1] C. Altomare, T. Suzuki, X. Chen, T. Verwaest, A. Kortenhaus, Wave overtopping of sea dikes with very shallow foreshores, Coast. Eng. 116 (2016) 236–257. http://dx.doi.org/10.1016/j.coastaleng.2016.07.002.

[2] E. Blayo, L. Debreu, Revisiting open boundary conditions from the point of view of characteristic variables, Ocean Model. 9 (2005) 231–252. http://dx.doi.org/10.1016/j.ocemod.2004.07.001.

[3] M. Zijlema, Modelling wave transformation across a fringing reef using SWASH, in: Proceedings 33th International Conference Coastal Engineering, 2012.

[4] T. Verwaest, T. Vanpoucke, P. Willems, M. De Mulder, Waves overtopping a wide-crested dike, in: Proceedings of the 32nd International Conference Coastal Engineering, 2010.

[5] T. Suzuki, S. De Roo, C. Altomare, G. Zhao, G.K. Kolokythas, M. Willems, T. Verwaest, F. Mostaert, Toetsing kustveiligheid-2015 - Methodologie: toetsings-methodologie voor dijken en duinen, Versie 10, Waterbouwkundig Laboratorium, Antwerpen, 2016.

[6] P. Smit, M. Zijlema, G. Stelling, Depth-induced wave breaking in a non-hydrostatic, near-shore wave model, Coast. Eng. 76 (2013) 1–16. http://dx.doi.org/10.1016/j.coastaleng.2013.01.008.

[7] G.S. Stelling, S.P.A. Duinmeijer, A staggered conservative scheme for every Froude number in rapidly varied shallow water ows, Int. J. Numer. Methods Fluids (2003) 1329–1354.

[8] T. Pullen, N.W.H. Allsop, A. Kortenhaus, H. Schüttrumpf, P. Troch, J.W. Van der Meer, EurOtop⟨www.overtopping-manual.com⟩, 2007.

[9] M.R.A. van Gent, Physical Model Investigations on Coastal Structures with Shallow Foreshores: 2D Model Tests with Single and Double-peaked Wave Energy Spectra, 1999.

[10] Y. Goda, Derivation of unified wave overtopping formulas for seawalls with smooth, impermeable surfaces based on selected CLASH datasets, Coast. Eng. 56 (2009) 385–399. http://dx.doi.org/10.1016/j.coastaleng.2008.09.007.

[11] H. Mase, M. Asce, T. Tamada, T. Yasuda, T.S. Hedges, M.T. Reis, Wave Runup Overtopping Seawalls Built Land Very Shallow Water, 2013, pp. 346–357. doi: ⟨http://dx.doi.org/10.1061/(ASCE)WW.1943-5460.0000199⟩.

[12] J. van der Meer, T. Bruce, New physical insights and design formulas on wave overtopping at sloping and vertical structures, J. Waterw. Port. Coast. Ocean Eng. (2014) 1–18. http://dx.doi.org/10.1061/(ASCE)WW.1943-5460.0000221.

[13] B.D. Rogers, M. Morellec, P.K. Stansby, A. Skillen, Incompressible smoothed particle hydrodynamics (ISPH) modelling of breakwater overtopping, in: Proceedings of the 34th International Conference Coastal Engineering, 2014.

[14] T.C.A. Oliveira, A. Sanchez-Arcilla, X. Gironella, Simulation of wave overtopping of maritime structures in a numerical wave flume, J. Appl. Math. (2012). http://dx.doi.org/10.1155/2012/246146.

[15] D.M. Ingram, F. Gao, D.M. Causon, C.G. Mingham, P. Troch, Numerical investigations of wave overtopping at coastal structures, Coast. Eng. 56 (2009) 190–202. http://dx.doi.org/10.1016/j.coastaleng.2008.03.010.

[16] S. Shao, C. Ji, D.I. Graham, D.E. Reeve, P.W. James, A.J. Chadwick, Simulation of wave overtopping by an incompressible SPH model, Coast. Eng. (2006) 723–735. http://dx.doi.org/10.1016/j.coastaleng.2006.02.005.

[17] D.E. Reeve, a Soliman, P.Z. Lin, Numerical study of combined overflow and wave overtopping over a smooth impermeable seawall, Coast. Eng. 55 (2008) 155–166. http://dx.doi.org/10.1016/j.coastaleng.2007.09.008.

[18] T. Li, P. Troch, J. De Rouck, Wave overtopping over a sea dike, J. Comput. Phys. 198 (2) (2004) 686–726. http://dx.doi.org/10.1016/j.jcp.2004.01.022.

[19] T.Q. Tuan, H. Oumeraci, A numerical model of wave overtopping on seadikes, Coast. Eng. 57 (2010) 757–772. http://dx.doi.org/10.1016/j.coastaleng.2010.04.007.

[20] A.J.C. Crespo, J.M. Domínguez, B.D. Rogers, M. Gómez-Gesteira, S. Longshaw, R. Canelas, R. Vacondio, A. Barreiro, O. García-Feal, DualSPHysics: open-source parallel CFD solver based on Smoothed Particle Hydrodynamics (SPH), Comput. Phys. Commun. 187 (2015) 204–216. http://dx.doi.org/10.1016/j.cpc.2014.10.004.

[21] N. Kobayashi, A. Wurjanto, Wave overtopping on coastal structures, J. Waterw. Port. Coast. Ocean Eng. 115 (1989) 235–251.

[22] J.B. Shiach, C.G. Mingham, D.M. Ingram, T. Bruce, The applicability of the shallow water equations for modelling violent wave overtopping, Coast. Eng. 51 (2004) 1–15. http://dx.doi.org/10.1016/j.coastaleng.2003.11.001.

[23] P.K. Stansby, T. Feng, Surf zone wave overtopping a trapezoidal structure: 1-d modelling and PIV comparison, Coast. Eng. 51 (2004) 483–500. http://dx.doi.org/10.1016/j.coastaleng.2004.06.001.

[24] K. Hu, C.G. Mingham, D.M. Causon, Numerical simulation of wave overtopping of coastal structures using the non-linear shallow water equations, Coast. Eng. 41 (2000) 433–465.

[25] M. Tonelli, M. Petti, Numerical simulation of wave overtopping at coastal dikes and low-crested structures by means of a shock-capturing Boussinesq model, Coast. Eng. 79 (2013) 75–88. http://dx.doi.org/10.1016/j.coastaleng.2013.04.007.

[26] Y. Yamazaki, Z. Kowalik, K.F. Cheung, Arterial fluid mechanics modeling with the stabilized space – time fluid – structure interaction technique, Int. J. Numer. Methods Fluids (2009) 473–497. http://dx.doi.org/10.1002/fld.

[27] G. Ma, F. Shi, J.T. Kirby, Shock-capturing non-hydrostatic model for fully dispersive surface wave processes, Ocean Model 43–44 (2012) 22–35. http://dx.doi.org/10.1016/j.ocemod.2011.12.002.

[28] H. Cui, J.D. Pietrzak, G.S. Stelling, Improved efficiency of a non-hydrostatic, unstructured grid, finite volume model, Ocean Model 54–55 (2012) 55–67. http://dx.doi.org/10.1016/j.ocemod.2012.07.001.

[29] M. Antuono, M. Brocchini, Beyond Boussinesq-type equations: semi-integrated models for coastal dynamics, Phys. Fluids 25 (2013). http://dx.doi.org/10.1063/1.4774343.

[30] M. Zijlema, G. Stelling, P. Smit, SWASH: an operational public domain code for simulating wave fields and rapidly varied flows in coastal waters, Coast. Eng. 58 (2011) 992–1012. http://dx.doi.org/10.1016/j.coastaleng.2011.05.015.

[31] M. Zijlema, G.S. Stelling, Further experiences with computing non-hydrostatic free-surface ows involving water waves, Int. J. Numer. Methods Fluids (2005) 169–197.

[32] D.P. Rijnsdorp, M. Zijlema, Simulating waves and their interactions with a restrained ship using a non-hydrostatic wave-flow model, Coast. Eng. 114 (2016) 119–136. http://dx.doi.org/10.1016/j.coastaleng.2016.04.018.

[33] E.P.D. Mansard, E.R. Funke, The measurement of incident and reflected spectra using a least squares method, in: Proceedings of the 17th International Conference on Coastal Engineering (ICCE 1980), 1980, pp. 154–172.

[34] H.E. Williams, R. Briganti, T. Pullen, The role of offshore boundary conditions in the uncertainty of numerical prediction of wave overtopping using non-linear shallow water equations, Coast. Eng. 89 (2014) 30–44. http://dx.doi.org/10.1016/j.coastaleng.2014.03.003.

[35] A. Romano, G. Bellotti, R. Briganti, L. Franco, Uncertainties in the physical modelling of the wave overtopping over a rubble mound breakwater: the role of the seeding number and of the test duration, Coast. Eng. 103 (2015) 15–21. http://dx.doi.org/10.1016/j.coastaleng.2015.05.005.

[36] K. Van Doorslaer, J. De Rouck, S. Audenaert, V. Duquet, Crest modi fi cations to reduce wave overtopping of non-breaking waves over a smooth dike slope, Coast. Eng. 101 (2015) 69–88. http://dx.doi.org/10.1016/j.coastaleng.2015.02.004.

[37] N.W.H. Allsop, T. Bruce, J. De Rouck, A. Kortenhaus, T. Pullen, H. Schüttrumpf, P. Troch, J.W. Van, der Meer, B. Zanuttigh, EurOtop II⟨www.overtopping-manual.com⟩, 2016.

[38] D.H. Peregrine, S.M. Williams, Swash overtopping a truncated plane beach, J. Fluid Mech. 440 (2001) 391–399. http://dx.doi.org/10.1017/S002211200100492X.

[39] W. Veale, T. Suzuki, T. Spiesschaert, T. Verwaest, F. Mostaert, SUSCOD Pilot 1: Wenduine Wave Overtopping Scale Model: interim Results Report. Version 2_0, Flanders Hydraulics Research, 2011.

[40] X. Chen, B. Hofland, C. Altomare, T. Suzuki, W. Uijttewaal, Forces on a vertical wall on a dike crest due to overtopping flow, Coast. Eng. 95 (2015) 94–104. http://dx.doi.org/10.1016/j.coastaleng.2014.10.002.

[41] The SWASH team, SWASH user manual: SWASH version 3.14A, 2016.

[42] M. Zijlema, G.S. Stelling, Efficient computation of surf zone waves using the nonlinear shallow water equations with non-hydrostatic pressure, Coast. Eng. 55 (2008) 780–790. http://dx.doi.org/10.1016/j.coastaleng.2008.02.020.

[43] J.M. Alsina, I. Cáceres, Sediment suspension events in the inner surf and swash zone. Measurements in large-scale and high-energy wave conditions, Coast. Eng. 58 (2011) 657–670. http://dx.doi.org/10.1016/j.coastaleng.2011.03.002.

[44] M.R.A. van Gent, Wave runup on dikes with shallow foreshores (2001.127254-262) J. Waterw. Port. Coast. Ocean Eng. (2001) 254–262.

[45] M. Antuono, L. Soldini, M. Brocchini, On the role of the Chezy frictional term near the shoreline, Theor. Comput. Fluid Dyn. 26 (2012) 105–116. http://dx.doi.org/10.1007/s00162-010-0220-8.